

SECRET [REDACTED]

COPY [REDACTED]

FEASIBILITY STUDY FINAL REPORT

**GEODETTIC ORBITAL
PHOTOGRAPHIC
SATELLITE SYSTEM**

VOLUME 3 DATA PROCESSING, PART 1

JUNE 1966

Declassified and Released by the N R O

In Accordance with E. O. 12958

on NOV 26 1997

SECRET [REDACTED]

SECRET

Copy No.

FEASIBILITY STUDY FINAL REPORT

**GEODETTIC ORBITAL
PHOTOGRAPHIC
SATELLITE SYSTEM**

VOLUME 3 DATA PROCESSING, PART 1

JUNE 1966

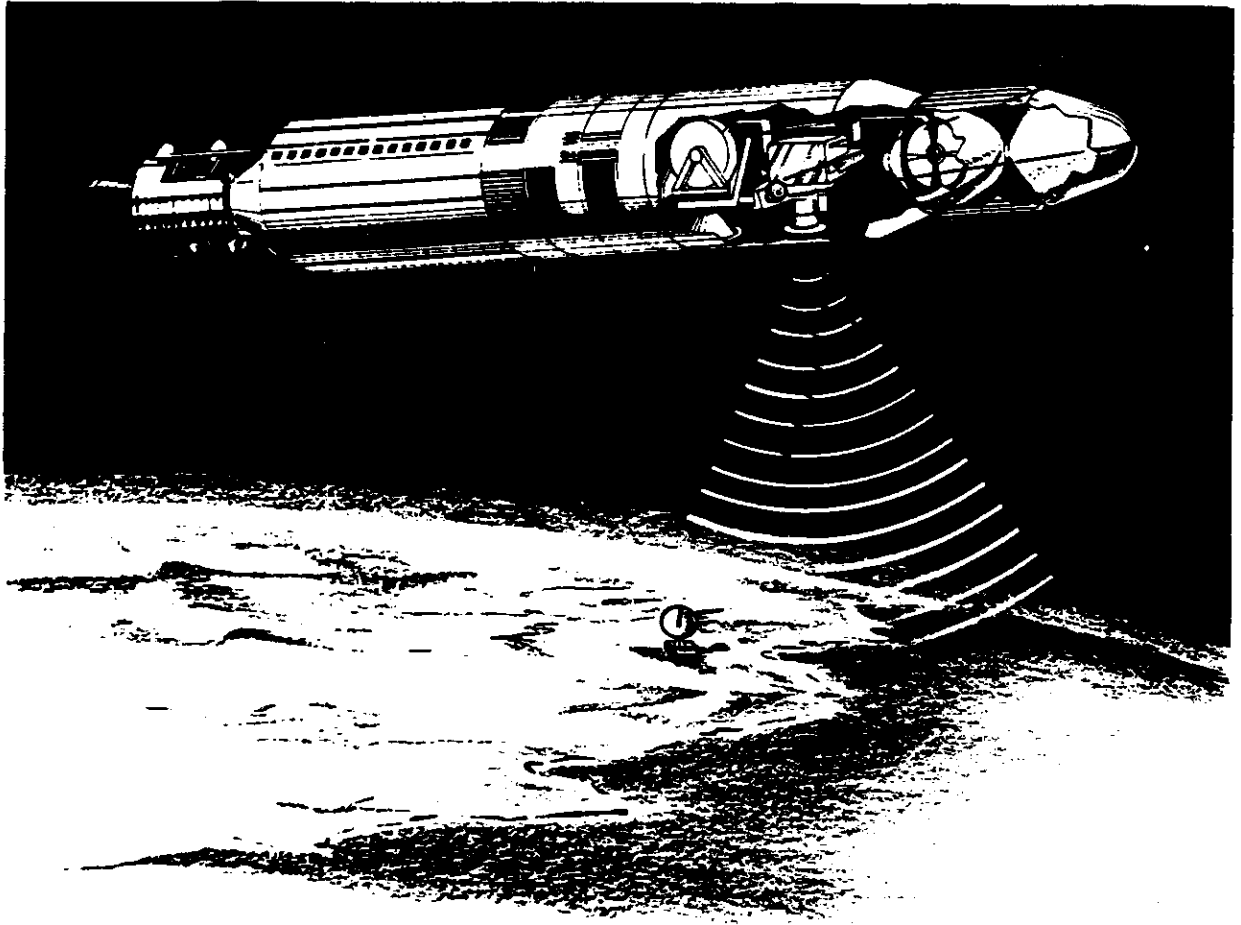
Itek

ITEK CORPORATION LEXINGTON 73

SECRET

VOL 3
9

SECRET



Geodetic Orbital Photographic Satellite System

SECRET

CONTENTS

	Page
3.1	Introduction 3-1
3.1.1	Photogrammetric Study Objectives 3-3
3.1.2	Photogrammetric Study Description 3-3
3.2	Residual Data Extraction Errors 3-5
3.2.1	Residual Film Distortion Errors 3-5
3.2.1.1	Permanent Film Distortions 3-6
3.2.1.2	Nonpermanent Film Distortions 3-6
3.2.1.3	Calibration Marks 3-7
3.2.1.4	Recommendations 3-9
3.2.2	Residual Refraction Errors 3-9
3.2.3	Residual Camera Calibration Errors 3-11
3.2.4	Residual Aberration Errors 3-12
3.2.5	Residual Mensuration Errors 3-13
3.2.6	Conclusions 3-14
3.3	Theoretical Photogrammetric Analysis 3-17
3.3.1	Introduction 3-17
3.3.1.1	Notation and Definitions 3-17
3.3.1.2	Rectangular Coordinates (XYZ) of Body 3-19
3.3.2	Camera Orientation 3-19
3.3.3	Constrained Solution 3-21
3.3.3.1	Least Squares Solution 3-21
3.3.3.2	Application and Extension 3-24
3.3.3.3	Error Propagation 3-29
3.3.3.4	Auxiliary Data 3-30
3.3.4	Detailed Formulation 3-31
3.3.5	Weighting Procedures 3-35
3.4	Photogrammetric Computations and Analysis 3-37
3.4.1	Operational Design 3-37
3.4.1.1	Overlap Program 3-39
3.4.1.2	Format and Resolution Program 3-42
3.4.1.3	Summary of Operational Procedures 3-43
3.4.2	Single Model Studies 3-43
3.4.2.1	Photogrammetric Errors on Landmark Locations 3-45
3.4.2.2	Orbital Errors in Landmark Location 3-47
3.4.2.3	Relative Errors in Centroid Location 3-48
3.4.2.4	Final Analysis and Summary of Single Model Studies 3-51
3.4.3	Strip Triangulation Studies 3-51

	Page
3.4.3.1	Triangulation Study Description 3-53
3.4.3.2	Analysis of Triangulation Data 3-56
3.4.3.2.1	Orbital Elements and Camera Positions 3-56
3.4.3.2.2	Landmark Locations 3-59
3.5	Substantiating Studies 3-73
3.5.1	Coordinate Systems 3-73
3.5.1.1	Introduction 3-73
3.5.1.2	Terrestrial Systems 3-73
3.5.1.3	Celestial Systems 3-74
3.5.1.4	Orbital Systems 3-77
3.5.1.5	Conclusion 3-78
3.5.2	Time Systems 3-78
3.5.2.1	Ephemeris Time 3-78
3.5.2.2	Atomic Time 3-79
3.5.2.3	Astronomical Time 3-79
3.5.3	Frequency Standards 3-80
3.5.4	Accuracies of Star Catalogs 3-81
3.6	Reseau Spacing 3-91
3.7	Conclusions 3-95
3.8	Bibliography 3-99
3.8.1	Film Distortion 3-99
3.8.2	Instrument Calibration and Errors 3-99
3.8.3	Aberration 3-100
3.8.4	Camera Calibration Techniques 3-100
3.8.5	Refraction 3-100
3.8.6	Analytical Photogrammetry and Miscellaneous 3-101
3.9	Mapping Capabilities 3-103
3.9.1	General Mapping Requirements 3-103
3.9.2	Mapping Specifications 3-104
3.9.2.1	Vertical Accuracies 3-104
3.9.2.2	Horizontal Accuracies 3-104
3.9.3	Geodetic Accuracy 3-104
3.9.4	Cartographic Accuracy 3-106
3.9.5	Map Information Content 3-107
3.10	Ground Handling of Mission Photography 3-109

TABLES

	Page
3-1 Recommended Environmental Controls	3-8
3-2 Standard Errors of Photo Measurements, as a Function of Resolution (n) or Image Diameter (d)	3-15
3-3 Expected Residual Errors After Applying Systematic Corrections	3-16
3-4 Glossary of Special Terms	3-38
3-5 Average Standard Errors in Point Determination	3-41
3-6 Variances of Orientation Elements, Radians ²	3-44
3-7 Standard Errors of Ground Point Determinations, Meters (Normalized 160 Nautical Miles)	3-44
3-8 Lens Resolution Data	3-44
3-9 Average Photogrammetric Errors on Landmark Location	3-46
3-10 Average Landmark Errors With Varying Orbital Covariance Matrix at 160 Nautical Miles	3-49
3-11 Standard Errors Furnished by Covariance Matrix of Centroid	3-49
3-12 Accuracy of Camera Station Determinations	3-52
3-13 Computational Scheme	3-54
3-14 Computational Scheme	3-55
3-15 Comparison of Standard Errors of Orbital Elements	3-58
3-16 Maximum Camera Station Location Errors for 160-Nautical Mile Altitude	3-58
3-17 Maximum Errors in Landmark Location at an Altitude of 160 Nautical Miles (Imaged on Three Photographs)	3-60
3-18 Positional Mode, Camera Station Errors in Geocentric Coordinates (H = 160 Nautical Miles)	3-61
3-19 Positional Mode, Camera Station Errors in Geocentric Coordinates (H = 160 Nautical Miles)	3-62
3-20 Covariance Matrices of Orbital Elements Determined From Strip Triangulations	3-63
3-21 Constrained Extension in Orbital Mode at 160 Nautical Miles	3-64
3-22 Constrained Bridge in Orbital Mode at 160 Nautical Miles	3-65
3-23 Ground Point Location Errors Constrained Extension in Positional Mode at 160 Nautical Miles	3-66
3-24 Ground Point Location Errors Constrained Bridge in Positional Mode at 160 Nautical Miles	3-67
3-25 Ground Point Location Errors Unconstrained Bridge in Positional Mode (H = 160 Nautical Miles)	3-68
3-26 Uncontrolled Orbitally Constrained Three Photo Model at 160 Nautical Miles	3-69
3-27 Uncontrolled Positionally Constrained Three Photo Model at 160 Nautical Miles	3-70

	Page
3-28 Stellar Distribution Accuracies of Major Star Catalogs	3-90
3-29 Maximum Number of Model Triangulations Meeting Landmark Specifications	3-97
3-30 Mapping Specification	3-105



FIGURES

	Page
3-1 Geometry of Atmospheric Refraction	3-10
3-2 Orbital Elements	3-18
3-3 Control Point Location	3-40
3-4 Internal Model Coordinate Errors at 160-Nautical Mile Altitude.	3-50
3-5 Location of Ground Points for Strip Triangulations	3-71
3-6 Frequency Diagram of SAO Position Errors	3-89
3-7 Ground Handling of Mission Photography, Block Diagram	3-110



SECRET

PREFACE

The objective of the Geodetic Orbital Photographic Satellite System (GOPSS) is to accurately determine the location of landmarks widely distributed over the earth's surface and provide better information concerning the geophysical parameters which affect this system and other systems operating at similar altitudes. The means chosen to accomplish this objective is to orbit a series of data acquisition systems supported by ground-based instrumentation. The data gathered by this system is incorporated into a sophisticated data reduction scheme which determines the geodynamic parameters and landmark locations.

Detailed studies were conducted to determine the feasibility of the GOPSS. The study period was designated as Phase I, and the results of these studies have been compiled into five volumes for reader convenience.

This volume considers the photogrammetric data subject to constraints imposed by orbital and auxiliary data, the mapping capabilities of the system, and ground handling of mission photography.

The division of the remaining volumes and their content are now briefly described for information and reference purposes.

Volume 1, Program Compendium and Conclusions, was prepared to provide briefly the details essential to a comprehensive understanding of the effort conducted during Phase I of the GOPSS feasibility study. System concept and objectives are described plus conclusions which concern the attainment or modification of the initial objectives, along with recommendations for a system configuration and a solution of the attendant data handling problems.

Volume 2, Data Collection Systems, describes the effort for implementation of the data acquisition requirements for the GOPSS program. This volume presents the preliminary design which defines and describes the various sensors, considers their functional interdependencies, and shows their evolution into an integrated GOPSS.

Volume 4, Data Processing, Part 2, discusses orbital considerations affecting the feasibility of the GOPSS. Physical models and computational procedures are reviewed and error studies involving typical sensors and model inaccuracies are described. Based on these studies, recommendations are made for tracking networks, auxiliary on-board sensors, and detailed orbit plans. In addition, the data reduction procedure, whereby the acquired data are simultaneously located to yield geodynamic parameters and landmark locations is considered.

Volume 5, Phase II-V Program Plan, describes the planning activity as it has been programmed through Phases II to V for the engineering, fabrication, and operational support for the delivery of five systems. Continuing studies which are required are also defined in this volume.

SECRET

SECRET

SUMMARY

The basic objective of the photogrammetric study was to evaluate the accuracy of positioning landmarks, well distributed over the earth's surface, with respect to a World Geodetic System. In order to accomplish that objective, prerequisite studies were conducted which showed:

1. Measured photographic data can be corrected for systematic errors, such that the residual errors in the corrected measurements due to calibration, film distortion, etc., are maintained to a maximum value of ± 4 microns at the 1-sigma level. This fact is predicated on the use of a prescribed 12-inch focal length lens, and the lens design and its performance characteristics that were generated during the program.
2. That the optimum reseau spacing, assisting the suppression of these errors to the ± 4 -micron level is 1 centimeter.
3. That the accuracy can be evaluated with which the camera exposure stations may be photogrammetrically determined with respect to the centroid of five landmarks imaged on three adjacent frames.

A theoretical photogrammetric analysis in which the mathematical model for the numerical evaluation of the photographic subsystem is developed. The accuracy with which landmarks can be determined from the reduced photographic data is considered in two segments.

1. The first of these evaluates the accuracy with which landmarks can be determined with respect to the orbit over unknown areas. It is concluded that landmark errors in the order of ± 39 feet cross-track, ± 42 feet in-track can be obtained and that the inclusion of a radar altimeter in GOPSS will reduce elevation errors to the order of ± 42 feet when operating at an altitude of 160 nautical miles.
2. The second segment deals with the accuracy of extending geodetic control from known areas by the method of aerial triangulation. It is concluded that the maximum length of such triangulations that ensure the elevation errors are less than ± 40 feet is 640 nautical miles for a vehicle altitude of 160 nautical miles.

The ground handling of the recovered mission photography is discussed, and concludes that the handling of these records presents no serious difficulty with existing equipment.

The final consideration is that of utilizing the GOPSS photography as a mapping medium. It is concluded that for medium scale maps, in the order of 1:200,000, that the criteria for Class A maps can be met. In order that large scale maps, of 1:100,000 scale or better, can be produced consistent with the mapping criteria, supplemental data must be provided to reduce the elevation errors and to increase the relative accuracies.

SECRET

SECRET [REDACTED]

Section A

PHOTOGRAMMETRIC ANALYSIS

SECRET [REDACTED]

SECRET

3.1 INTRODUCTION

The mission of the Geodetic Orbital Photographic Satellite System (GOPSS) involves the location of landmarks over the earth's surface to high accuracies from data collected by an orbiting vehicle and the simultaneous accurate evaluation of the geodynamic parameters which influence the motion of the orbiting vehicle. The principal data gathering system for landmark location is photogrammetric, and consists of a set of cameras, one to photograph the earth's surface and two stellar cameras to define orientations. Orbit position is defined by typical tracking networks, re-enforced by selective photogrammetric data. Accurate time in orbit is recorded and auxiliary onboard sensors may be employed.

The GOPSS program might be treated as two independent calculating schemes. The first is the utilization of tracking data as the prime input to determine the orbit; the second is the use of this orbit to position the camera stations from which the location of ground points is obtained. In this positioning task, the camera is considered as the prime sensor, so that the production of a landmark catalog is approached as if it were a photogrammetric problem alone.

This leads to an approach which treats each of the data types according to independent data reduction schemes and can become involved, since functional relationships exist between the various types of data despite the fact that they are independently acquired. For example, ground tracking data provide the most accurate information for the determination of orbital parameters, yet these parameters can be weakly determined from the photogrammetric solution. The independent reduction of ground tracking data and photographic records is theoretically unsound, since these two sets should be consistent with each other through on common factors, namely, the orbital parameters.

Investigating the feasibility of the GOPSS concept using an integrated treatment as described in Volume 4, Section 4.12 requires the complete data reduction scheme that will be necessary to finally reduce the data from the GOPSS. Only partially integrated analyses can be performed in this study. If, by proceeding in this manner, it is concluded that meeting the specification is feasible, then the final data reduction involving complete integration would more strongly re-enforce this conclusion.

In the past, multidata systems have been considered as being composed of a prime sensor that fulfills the basic system objective, and various auxiliary sensors that support and complement the prime sensor. The role assigned to the so-called auxiliary systems has been to provide supplemental information and facilitate the data reduction problem. Nowadays, auxiliary data systems frequently provide better quality and a greater quantity of data than that furnished by the prime sensor. This has led to a revision in the concepts of auxiliary data utilization, such that all related data are used to perform an integrated and simultaneous adjustment to obtain consistent results in achieving the system objectives.

SECRET

SECRET

This section of the report is directed toward evaluating the photogrammetric accuracies that can be attained as well as furnishing realistic estimates of the expected input errors to the orbital computations. It is recognized that providing these error estimates implies that the reduction of photogrammetric and orbit tracking data are independently performed. This conflicts with the preceding comments, but is necessitated by the structural organization of this phase of the study. The recommended data reduction scheme, however, will not consist of independent computational schemes, since the combined data acquisition capability of the system provides for a great amount of over-determination of the desired information, even for small orbital segments, so that a constrained adjustment will be mandatory to achieve optimum results.

As previously stated, the GOPSS program can be treated as utilizing tracking data to determine the orbit, and using this orbit to position the camera stations from which the location of ground points are obtained. However, since the camera stations lie on the orbit, inconsistencies will result unless the photogrammetric data are used with the other data in determining the orbital parameters. In this regard, and provided that a sufficiency of ground control points exists, the photographic records furnish a means of determining discrete orbital positions. These positions must conform to those that can be interpolated from an alternate orbit determination, and thus a condition is imposed on the data adjustment. The whole purpose of this adjustment is to eliminate the discrepancies that would otherwise exist, so that no matter whether one determines camera positions photogrammetrically or by using orbital positions, the same location results. The same holds true for landmark determination—after adjustment, the coordinates of such points should be the same, whether resulting from a long photogrammetric strip triangulation or compiled from two exposures whose locations have been orbitally determined.

In this portion of the analysis, the camera positioning and landmark location requirements will be treated as a photogrammetric problem, subject to functional restraints and constrained to various auxiliary and orbit tracking data. This assigns the photogrammetric subsystem the primary role. However, this is only a specific aspect of the overall data reduction scheme, and, provided that the correct functional relationships are enforced, it is irrelevant. In other words, the same data could be equally viewed as an orbit determination in which the photogrammetric data are a minor set of tracking information.

The use of auxiliary data as an integral part of the photogrammetric reduction is one of the strengths of the GOPSS. Individual photogrammetric models possess a reasonable geometric strength. The conjunction of successive models, however, to form a triangulated strip, is subject to an unfavorable error propagation. It is this fact which precludes the attainment of the objectives through photogrammetric techniques alone. These techniques do not have the strength to extend positional control into uncontrolled areas even with such a highly sophisticated camera as this, but must depend on a stable and well-defined orbit determined by other sensors. Additional data, acquired by other sensors, when incorporated into the triangulation with the correct functional constraints suppress the error accumulation to a surprisingly small minimum.

The other considerations in this study consists of a sequence of single and multimodel triangulations. Although it might appear as if this were the whole concern of this study, this is far from the truth. Essentially, the triangulations are performed to determine whether certain system objectives can be achieved, and to demonstrate that the proper use of auxiliary data enables these objectives to be surpassed. Since these triangulations require ground control data in the initial model as a minimum, some consideration of the quality of these points is necessary. The basic assumption has been that the location errors of control points i.e., photo-identifiable ground points whose positions are known, are uncorrelated, and equal to a spherical error of

SECRET

± 10 meters. This is a typical internal error value that could be encountered in existing high quality geodetic nets. The specific problem of the errors between distinct geodetic systems necessitates that a datum shift for each geodetic net be incorporated into the data reduction scheme. In general, such shifts with respect to a world geodetic system might be expected to be as much as 50 meters. Although the determination of these shifts is the basic objective of the DOD satellite triangulation program (PAGEOS), it is also an incidental accomplishment of the GOPSS program. These aspects are discussed in some detail in this volume and in Volume 4.

3.1.1 Photogrammetric Study Objectives

The basic objective of this photogrammetric study was to evaluate the accuracy of positioning landmarks, well distributed over the earth's surface, with respect to a World Geodetic System.

In order to accomplish this objective, various prerequisite studies were conducted, which permitted the evaluation of some intermediate objectives. These studies showed:

1. That the measured photographic data can be corrected for systematic errors, such that the residual errors in the corrected measurements due to calibration, film distortion, etc., are maintained to a maximum value of ± 4 microns at the 1-sigma level. This is predicated on the use of a prescribed 12-inch focal length lens, and the lens design and its performance characteristics that were generated during the program.
2. That the optimum reseau spacing, assisting the suppression of these errors to the ± 4 -micron level should be determined.
3. That the accuracy can be evaluated with which the camera exposure stations may be photogrammetrically determined with respect to the centroid of five landmarks imaged on three adjacent frames.

Before discussing the specific analyses, a general description of the overall study is given below.

3.1.2 Photogrammetric Study Description

Section 3.2 consists of an examination of the systematic errors affecting the recorded and extracted photographic data, and the corrections necessary for their removal from the measured coordinates. Since it is frequently not possible to exactly define the systematic errors and their corrections, residual errors are expected to exist in the refined coordinates. These residual errors are the basic inaccuracies present in the photogrammetric data input into the computational schemes.

The most significant of the systematic errors, mechanical film distortions, can be reduced by the use of a reseau. The reseau spacing necessary to suppress the effects of the residual errors to a specified tolerance is described in Section 3.6.

Section 3.3 consists of a theoretical photogrammetric analysis in which the mathematical model for the numerical evaluation of the photographic subsystem is developed. This analysis is directed toward the overall data reduction scheme in which auxiliary data, prime orbital data, etc., are simultaneously incorporated.

These two portions of the study were accomplished through an extensive literature search, discussions with several of the authors, and a certain amount of original work.

SECRET [REDACTED]

Section 3.4 consists of a sequence of numerical analyses, utilizing the model developed in the second phase. Basically, the photographs were either statistically constrained to discrete orbital positions, or functionally constrained to orbital positions and utilized stellar orientations.

The numerical analyses that were performed established the following design parameters and attainable accuracies:

1. The optimum overlap between successive photographs, with the incidental determination of the effects of varying the weights assigned to the measured photocoordinates (Section 3.4.1.1)
2. The effects of decreasing the length of the format on the attainable photogrammetric accuracy (Section 3.4.1.2)
3. The determination of the accuracy of locating camera positions with respect to the centroid of five landmarks imaged on three adjacent frames with the incidental determinations of the effects of varying the orbital covariance matrix (Section 3.4.2)
4. The attainable accuracy of strip triangulations, as bridges and extensions, assuming ground control data (Section 3.4.3)
5. The attainable accuracy of positioning landmarks from orbitally constrained photography, with no ground control (Section 3.4.1.1, Table 3-11).

The last three sets of numerical studies were repeated at three different altitudes, namely, at 120, 160, and 200 nautical miles, in order that the effects of increasing the altitude on the system performance could be evaluated.

SECRET [REDACTED]

3.2 RESIDUAL DATA EXTRACTION ERRORS

This section is concerned with examining the fundamental accuracy with which data extracted from the photographic records can be refined through the removal of systematic errors.

The inaccuracy of these refined data is due in part to an inadequate knowledge or expression of the systematic errors and in part to the presence of random errors inherent in the extracted data.

This section considers the various systematic errors and provides estimates of the magnitudes of the residuals errors in the refined data. These estimates lead to the imposition of various conditions on the data extraction equipment, and the refining processes in order that measuring tolerances can be met.

A preliminary objective states that the reduced photo coordinates should be accurate to a 1-sigma level no greater than 4 microns. This is a total error that results from a combination of all the individual contributing errors. For this study, a linear error model is used, such that the residual error, σ_i , at any point, i , is expressed as

$$\sigma_i = [\sum \sigma_{ij}^2]^{1/2}$$

where the summation is over j , of the contributing errors at the point i .

The basis for selecting the linear model is based on the hypothesis that the individual errors are independent, and that the residual systematic errors are randomly distributed.

The various contributing residual errors, σ_i , are tabulated

- σ_1 = residual film distortion error
- σ_2 = residual refraction error
- σ_3 = residual camera calibration error
- σ_4 = residual aberration error
- σ_5 = residual mensuration error
- σ_6 = residual comparator calibration error

Each of these component errors is now individually considered.

3.2.1 Residual Film Distortion Errors

Perhaps the most serious problem involved in the reduction of photogrammetric measurements is the adequate removal of systematic film distortions. The usual methods of compensating for these distortions involve the use of either calibrated fiducial markers or a reseau, the images of which are recorded on the photography at the time of exposure.

Film distortions existing in photography cause image points to be displaced from instantaneously imaged locations. These displacements are primarily a function of the inherent characteristics of the film base, and of the developing procedures. Some of the distortions occur as a result of tensile forces applied to the imperfectly elastic roll film during its transport in the camera and in the developing and drying equipment. Other permanent distortions occur as a result of the manner in which the film is handled, developed, and dried. They are primarily caused by the release of stresses in the dry film and emulsion during development and by the compressive forces acting on and between the emulsion and film base during drying. Irregular random distortions are also present, the magnitudes of which determine a noise level or threshold, beyond which the application of adjustment procedures to measure photographic images is pointless.

3.2.1.1 Permanent Film Distortions

The original negatives are considered to have a format size of 9 by 18 inches. The film used is assumed to be an Estar base, 0.0025 inch thick, with a type SO-130 emulsion.

The high stiffness and low flow of the Estar base resist the tensile forces of the camera and processing equipment. Furthermore, the backing of the film causes the unbalance of forces during drying to be very small, so that the elastic compression is frozen in the film. The dimensional changes that can be expected as a result of processing may amount to 0.05 percent and those due to aging may be ignored.

For the selected format, this would cause total shrinkages as large as 228 microns in length and 114 microns in width. In the event that copy positives used in the measuring apparatus are made on a thick (0.007 inch) Estar base, which has a shrinkage factor of 0.02 percent, an additional shrinkage of 92 microns in length and of 46 microns in width will be present. Since these are systematic deformations, they are additive.

3.2.1.2 Nonpermanent Film Distortions

The most important factors causing these temporal variations are changes in the temperature and relative humidity of the film's environment. Although Estar base films possess excellent physical characteristics, only very small changes in temperature and humidity can be neglected. The coefficient of linear thermal expansion is $15 \times 10^{-6}/^{\circ}\text{F}$, and that of linear hygroscopic expansion is $35 \times 10^{-6}/1$ percent relative humidity. Thus, temperature changes of 1°F during the measuring period will cause a dimensional change of approximately 6 microns over an 18-inch length of film. The corresponding dimensional change for a 1 percent increase in humidity will be approximately 17 microns. Provided that the absolute humidity remains constant, these changes will tend to compensate each other, although the hysteresis of the film expansion with humidity may negate this compensation.

In addition to the dimensional changes induced by changes in the whole environment, local temperature and humidity variations may occur when the film is being measured. These are primarily due to the effect of concentrated light on that portion of the film which is being viewed and the heating effect of other electrical machine components. These local distortions may be difficult to detect and remove from the measurements.

It is often difficult to determine whether image displacements are caused by film distortion or by some other factor unrelated to the dimensional stability of film. Perhaps the most significant source of such displacements is lack of flatness in the camera (partially compensated for by

SECRET

using a reseau register glass in the focal plane of the camera). It appears to be impossible to separate the errors caused by this source from those caused by dimensional changes. Furthermore, lack of film flatness in reproduction and measuring equipment may occur unless very careful precautions are taken. Environmental conditions must be rigorously stabilized during the processing and measurement of film if accurate results are to be obtained. According to Michener, these environmental conditions should be maintained in the postdevelopment storage areas. The obvious solution would be to store the processed film in the same room that is used for the measuring equipment. This would mean that it would be necessary to environmentally control only one room. The environmental controls which is felt necessary to maintain in order to minimize the effects of atmospheric temperature and humidity changes are listed in Table 3-1.

The alternative to using original film or copy diapositives on a stable film base, is to make reproductions on coated glass plates.

Glass plates are superior to film base in all respects involving stability. Although the former are quite expensive when compared to a film base, an economic advantage is obtained when using glass since the cost of establishing the precise environmental controls for the storage and mensuration of film is not involved. Furthermore, by selecting the thinnest Grade I plates, substantial savings may be made. It may be argued that the lower flatness tolerance of these plates negates such an advantage. However, it should be noted that such plates are much flatter than a film base can be, and that the lack of flatness is unimportant when using an orthogonal viewing instrument.

Glass plates are easy to handle and rigidly attach to the measuring and reproduction machines. It is extremely difficult to secure film in such apparatus without applying tensile or compressive forces to the film. Such forces produce distortions which may defy evaluation.

It is therefore concluded that glass plates are to be preferred over a film base for use in a precise photogrammetric data reduction system. Copies of the original exposure should be made onto glass plates, thereby "freezing" the distortions existing at that time onto a permanent record. It has frequently been commented that the bulk of glass plates requires a large storage facility, however, a 9-inch by 18-inch glass plate 1/4 inch thick displaces a volume of 40.5 cubic inches. For 15,000 glass plates, this displacement is 351.5 cubic feet. Assuming that an equal volume is required for the crating and separation of these plates, a storage area of 700 cubic feet is required. This is not a significantly large storage requirement.

3.2.1.3 Calibration Marks

Normally, survey cameras are provided with four fiducial markers. These are located at either the four corners or at the midpoint of each side of the format. By comparing the measured distances between the marker images with their calibrated values, the effect of the systematic film distortion can be reduced to the extent that the standard residual error is about 20 microns (Tewinkel, 1960) to 15 microns (Laurila, 1961) for acetate base films. In the event that a stable Estar base film is used, the standard residual error is reduced to about 5 microns (Tewinkel, 1961; Adelstein, 1962).

A significant improvement in the compensation for systematic film distortion may be obtained if the survey camera is provided with additional calibrated markers. According to Tewinkel, 1961 and 1962, the use of eight markers, located at the four corners and at the midpoint of each side of the format, forces the discrepancies into smaller bounds so that the standard residual error is decreased by about one half ($2\frac{1}{2}$ microns). If a central mark is included, the effect of the nine marks is to reduce the standard residual error by one quarter (1.25 microns).

SECRET

Table 3-1 — Recommended Environment Controls

Environment*	Temperature, °F	Humidity, percent
Pre-exposure	70 ± 2	50 ± 5
Development	70 ± 1 to 2	—
Drying	70 ± 1 to 2	50 ± 2
Storage	70 ± 2	50 ± 5
Measuring†	70 ± 1 to 2	50 ± 1

*All environments are assumed to be dust free.

†If storage and measuring environments are difficult, ensure that the film is presoaked in the measuring environment for at least 24 hours. This should then be followed by a 4-hour instrumental soak period.

Substantial analyses by Brock and Faulds, Gimrada, et al., indicate that residual film distortion cannot be expected to be less than 1 to 2 microns. With the exception of some of the Gimrada studies, these analyses pertain to 9- x 9-inch format. Extrapolation to a 9- x 18-inch format is valid, provided that 12 fiducial marks and 3 central marks are imaged onto the film.

To ensure that a precise determination of the systematic film shrinkage is obtained, a calibrated reseau plate which is imaged on the negative at the instant of exposure will be used. It is pointed out that two different philosophies concerning the use of a reseau exist.

The first of these, implied by the preceding comments, is to use measures of the reseau point to determine an analytical expression for the systematic distortions. Since this may be adequately determined by an 8- to 10-parameter equation, a dense reseau spacing is unnecessary.

On the other hand, reseau marks may be considered to have their calibrated "exact" values and coordinates of image points determined by measuring and adjusting the incremental differences from surrounding reseau points. To prevent measuring and interpolating over long distances, a reseau spacing of 1 centimeter is recommended.

3.2.1.4 Recommendations

It is recommended that a reseau plate having a maximum density of 1 centimeter be used, so residual errors in the order of 1 to 2 microns are to be expected. The specific reseau technique to be used will be determined with regard to instrument and data reduction characteristics.

3.2.2 Residual Refraction Errors

The displacement of image rays due to atmospheric refraction may be corrected by applying various well known expressions. Owing to the dependency of most of the usual solutions on an accurate determination of the central angle, θ , and of the astronomic refraction, r_α , the strength of these solutions is somewhat variable.

The geometric situation for photogrammetric refraction, r_p , from a satellite-borne camera is illustrated by Figure 3-1. With reference to Figure 3-1

$$r_p = \alpha - \beta$$

$$\text{where } \tan \beta = \sin \theta \left[1 + \frac{H}{R} \cos \theta \right]^{-1}$$

in which

$$\theta = Z + r_\alpha - \alpha$$

and

$$\sin Z = \left[1 + \frac{H}{R} \right] \frac{\sin \alpha}{\mu_p}$$

μ_p being the index of refraction at the point P, which is appropriately determined from four terms of Garfinkel's model.

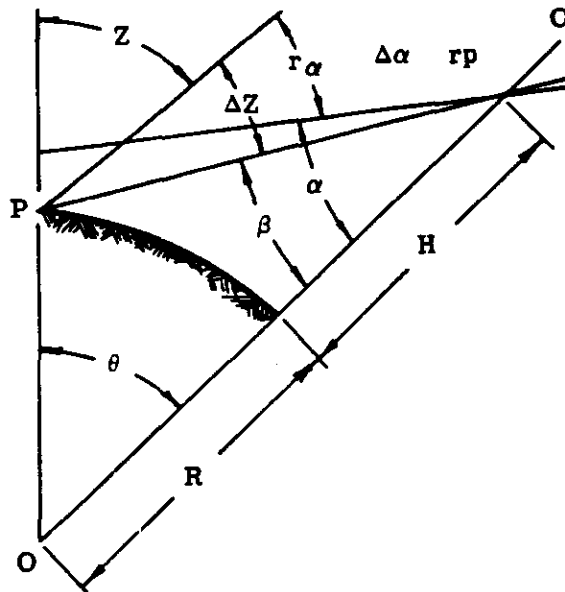


Fig. 3-1 — Geometry of atmospheric refraction

SECRET

It is seen that the photogrammetric refraction is a function of six dependent variables α , H , R , Z , r_α , and μ_p . Errors in these variables affect the accuracy of the photogrammetric refraction. Photogrammetric refraction is relatively unaffected by errors in the satellite height, the index of refraction, the zenith distance, and the radius of the earth. This has been discussed by Case, who shows that the sensitivity of photogrammetric refraction to error in the nadir angle, α , satellite height, H , earth radius, R , and index of refraction, μ_p , is so small that it may be considered negligible. However, the sensitivity to errors in astronomic refraction and in zenith distance is extremely high and cannot be ignored. Case recommends the use of the flat earth formula, thereby dispensing with the central angle, θ , which is simple to use but relatively insensitive to errors in all the variables. His implication is that the difficulty lies with the small central angle, θ .

Subsequent work by Schmid discusses the problem of refraction more extensively, and derives the following formula

$$r_p'' = \frac{2.330 \tan (180 - \alpha - \theta) \rho'' \cdot W}{H}$$

where W is a meteorological correction factor. Schmid presents tabulated data indicating the effects of completely neglecting the refraction problem, from which it is estimated that if the refraction is considered, the maximum residual error will not exceed 0.4 arc second, i.e., 0.6 micron, for the camera under consideration.

3.2.3 Residual Camera Calibration Errors

Advanced camera calibration techniques exist today which utilize photography of control fields made on glass plates and are capable of reducing the errors due to the distortions to the order of 1 to 2 microns. Such calibrations must necessarily be much more sophisticated than the usual consideration of radial lens distortion, and include parameters that account for tangential distortions, asymmetry of the distortions, lens decentering, etc. The most advanced of these calibrations are those of D. Brown, and of the USCGS, due to H. Schmid. Both are similar, being based on stellar photography, but differ in that Schmid's method is somewhat more sophisticated (carrying 23 parameters against Brown's 18). Both authors commendably apply generalized least square techniques in which appropriate weighting functions are applied to the input data, thereby enabling statistically valid estimates of error propagations to be formed. These methods are well documented, and need not be detailed here.

It is of interest to note that these methods are photographic, following the recommended practice of Commission I of the International Society of Photogrammetry. Since these recommendations further state that it is desirable for calibrations to be performed under conditions similar to the working environment of the camera system, it is perhaps worthwhile to consider the possibility of inflight calibration of the airborne cameras. Although preflight calibrations will be performed with the system, it is not unlikely that environmental conditions will affect the camera performance in some unknown manner, which can be detected only through inflight calibrations, (discussed in Volume 2). This calibration would require that the vehicle be rotated in such a manner that the terrain and stellar cameras both point into star fields, and that during the exposure time, the vehicles be in free flight. This can reasonably be accomplished during passage through the earth's shadow zone.

The great advantage of this inflight calibration is emphasized by the difficulties that exist in determining the camera constants for a near vacuum, and for recognizing any temporary change

SECRET

in the relative orientation of the stellar and terrain cameras. The reduction of these calibrations would be performed in the same manner as ground based calibrations.

3.2.4 Residual Aberration Errors

Aberration is the image displacement caused by the (relative) motion of the camera system during the time it takes for the image radiation to reach the recording medium from the receptor.

If the relative vehicle velocity is v , the angular deviation, A , due to aberration is

$$A = \frac{v}{C} \sin \theta$$

where C = velocity of light

θ = angle between the image-object vector and the velocity vector

Since A is a small angle, the image displacement, Δ , may be written as

$$\Delta = S_i A$$

where $S_i = (x_i^2 + y_i^2 + f^2)^{1/2}$

This displacement is parallel to the velocity vector. For a tilted photograph this displacement is reduced to

$$\Delta' = \Delta \cos t$$

provided the resultant tilt is not too large. For a primary rotation of ω and a secondary rotation ϕ , one obtains t as

$$t = \tan^{-1} [(\tan^2 \omega + \sin^2 \phi)^{1/2} (\cos \phi)^{-1}]$$

The resulting displacement of the images is resolved into the components parallel to the photo axes through the swing angle κ as

$$\delta x = \Delta' \cos \kappa$$

$$\delta y = \Delta' \sin \kappa$$

Since it has been assumed that tilts will be small, one may compute

$$\sin \theta = (x_i^2 + y_i^2)^{1/2} / S_i$$

with little significant error, to obtain

$$\delta x = v(x_i^2 + y_i^2)^{1/2} \cos \kappa \cos t / C$$

and

$$\delta y = v(x_i^2 + y_i^2)^{1/2} \sin \kappa \sin t / C$$

~~SECRET~~

Maximizing, i.e., putting $\kappa = t = 0$, one obtains

$$\delta x = v(x_i^2 + y_i^2)^{1/2}/C$$

For a velocity of $v = 7$ kilometers/second, and $C = 299,696$ kilometers/second

$$\delta x \sim 0.234 (x_i^2 + y_i^2)^{1/2} \times 10^{-4}$$

if

$$(x_i^2 + y_i^2)^{1/2} \sim 200 \text{ millimeters}$$

then

$$\delta x \sim 5\mu$$

This is a significant correction and should not be ignored. However, approximate values for all parameters in this correction may be used without causing any significant residual error.

3.2.5 Residual Mensuration Errors

The mensuration equipment used in extracting data from the photographic records must provide for a readout and least count of 1 micron and be calibrated by appropriate methods in order to attain the ultimate accuracy. The calibration of analytical instruments has greatly improved in recent years, as evidenced by the thoroughly documented techniques to be found in the technical literature.

According to Rosenfield, the application of these calibration data reduces the average standard error of the measured coordinates to ± 1.0 micron, which is due to the mensuration equipment alone. This agrees well with Gugel's data, who, using Rosenfield's technique, obtains standard errors in the order of 1.2 to 1.9 microns, and are not too different from those values determined by Hallert (± 2.5 microns) and Brown (± 2.3 microns).

A more sophisticated modification of this technique has been made by the Itek Data Analysis Center, which utilizes appropriate weighting techniques to obtain the variance-covariance matrix of the corrective parameters and enables one to determine the weight matrix of the corrected coordinates. The unit standard deviation of the reduced coordinates is in the order of 0.5 micron, due to the propagation of the errors in the calibration data. This precision is partly illusionary, since it is necessary to assign appropriate weighting functions to measured image coordinates in order to determine the final precision. The basic criterion for these weighting functions is the resolution.

Before discussing these functions, it is appropriate to comment on resolution.

Resolution when expressed in lines per millimeter, has frequently led to erroneous interpretation. The typical test chart consists of a series of equally spaced uniform lines on a contrasting background, in which the spaces between lines are equal to the line width. The minimum resolvable distance is thus equal to the width of a line, or space. For a resolution of n lines per millimeter, this means that $(1/2 n)$ millimeters is the minimum resolvable distance. From a theoretical point, it has been argued that the minimum resolvable distance is $1/(2n-1)$ millimeters, consisting of n lines separated by $n-1$ spaces, but here it is elected to use the value $1/2n$. In this respect,

~~SECRET~~

frequency spectra and transfer functions, although less easily understood, are less frequently misinterpreted.

Applying the minimum resolvable distance to determine the dimensions of the minimum object on the ground that can be imaged is not fully correct. This has been fully described by G. Brock, who states:

"As the camera moves away from the object, the image on the negative first grows smaller in accordance with the laws of geometrical optics, until its dimensions have reached the critical value below which the taking system cannot deliver a reproduction. As the distance between the camera and object is further increased, the size of the image remains approximately the same, but its contrast against the surrounding background diminishes. The distance at which a given object is still reproduced on the negative depends primarily on the contrast of the object, although the contrast (γ) of the negative material also has a certain influence. In this extreme case of the reproduction mode, the shape of the image produced is determined by the characteristics of the lens and is virtually independent of the object of photography."

The use of resolution as the criterion for weighting photographic coordinates is generally in agreement with current photogrammetric practice and theory. Extensive experiments have been made, and are still being made, to determine the most appropriate function of resolution to use. Unfortunately, no concurrence of opinion as to the best function to use has been reached, essentially due to the variation in contrast between the sets of experimental data and the absence of any thorough theoretical study of this problem. It has been established by Schmid, Blachut, et al., that well defined photo points and targeted stations can be measured with a precision that is in the order of 1/10th of the minimum resolvable element. For high contrast point sources, for example stellar plates, it is generally agreed that the pointing may be obtained with a precision approaching 1/20th the diameter of the image. However, as pointed out by Charman, no simple relationship exists between resolution and the measuring error.

Gardiner's data and his criterion are based on determining the absolute accuracy of mapping from air photography, in which low contrast imagery and frequently ill-defined images are characteristic.

His values include an inherent identification error that is always present in general mapping, except when well defined points are being measured. Furthermore, this criterion is to be applied to the mapping mode, a continual sequence of single pointings, not multiple independent pointings.

For reference purposes, the various weighting criteria have been listed in Table 3-2, with an attempt to classify them according to image contrast.

From these tabulated data, it is possible to select a standard error that varies between $\pm 0.025/n$ to $\pm 0.34/n$. In order that a reasonable weighting criterion might be used in the calculations, a value given by Ghosh ($\pm 0.075/n$) was selected.

3.2.6 Conclusions

Measured photographic coordinates are subject to two kinds of errors—systematic and random. The systematic errors may be accounted for by applying the appropriate corrections

~~SECRET~~

Table 3-2 — Standard Errors of Photo Measurements, as a Function of Resolution (n) or Image Diameter (d)

Point	Standard Error	Author
High contrast (stellar image)	$\pm 0.025/n$ millimeter (0.05 d)	Eichorn
Well defined photo point (target)	$0.05/n$ millimeter (0.1 d)	Schmid Blachut
Average contrast natural photo points	$0.04/n$ millimeter - $0.07/n$ (0.08 d - 0.14 d)	Ghosh Hallert
Low contrast photo points	$0.06/n$ - $0.2/n$ $0.166/n$	Lyon, et al. Charman
Average photo detail (mapping)	$0.34/n$	Gardiner

~~SECRET~~

for instrumental calibration, film shrinkage, camera calibration, refraction, and aberration. However, owing to the imperfect evaluation of these systematic errors, residual effects remain after their application. These are presumed to be accidental in nature.

The mensuration error is random and functionally related to resolution. It is therefore expedient to define a data extraction error that is random in nature and a combination of the effects of resolution, residual image motion, and residual mensuration errors.

According to the preceding sections, the systematic errors may be eliminated to yield residual accidental errors of the magnitudes shown in Table 3-3. To this total residual error of ± 2.7 microns, the residual extraction error, σ_e , must be applied to yield the final expected precision in the photographic coordinates. According to the system specifications that this should be no greater than ± 4 microns, the magnitude of the error, σ_e , cannot attain a value greater than ± 2.9 microns. This value, σ_e , is due to the image alone and is essentially a pointing and identification error. The question that must now be answered is whether this is a value that might reasonably be expected.

The tolerance can be met if one can apply a weighting function that is proportional to $0.09/n$ millimeter, since the minimum resolution of the camera system is in the order of 30 lines per millimeter.

When multiple readings of each image coordinate are made, the precision of the measurements increases as the square root of the number of pointings. In order to achieve a ± 4 -micron tolerance, a minimum of three pointings on each image point is necessary. This is in accordance with the standard operating procedures when making comparator measurements.

It is therefore concluded that the ± 4 -micron reduced photo coordinate tolerance can be met, provided that careful mensuration and reduction procedures be used, and that all equipment be associated with valid calibration parameters. However, in the numerical studies described in Section 3.4, it has been elected to use a value that is considerably worse than this 4-micron value, in order that our results should not be too optimistic.

Table 3-3 — Expected Residual Errors After Applying Systematic Corrections

	Residual Error	Magnitude, microns
σ_1	Film distortion	± 1.5
σ_2	Refraction	± 0.6
σ_3	Camera calibration	± 1.5
σ_4	Aberration	± 0.0
σ_5	Comparator calibration	± 0.5
—	Camera mechanisms	± 1.6
	Total residual error (RMS)	± 2.7

3.3 THEORETICAL PHOTOGRAMMETRIC ANALYSIS

3.3.1 Introduction

The objective of this section is to devise an appropriate mathematical model by means of which the photogrammetric aspects of the GOPSS program might be examined. In order that this examination might be efficient, it has been devised to incorporate auxiliary data and to propagate input errors through the computations into the output data. This error propagation is statistically sound, and enables one to perform a systems analysis using covariance methods rather than the laborious Monte Carlo techniques.

The selected error model will consider up to nine consecutive overlapping photographs, although in practice it is doubtful if nine consecutive exposures can be obtained. These nine photographs can be subject to orbital constraints and those imposed by auxiliary data. As a consequence of the limited extent of the orbital arc, a simple Keplerian model is assumed, which corresponds to the osculating ellipse at the midexposure time. It is pointed out that such a simple orbital model will not be used in the final data reduction scheme, but will include an extensive parameterization of the perturbing forces.

The theory presented here is sufficiently general and extensive to perform an analysis of the photogrammetric portion of the GOPSS. However, if long arc reductions are performed, as will be the case in the final data reduction scheme, there is no serious problem in modifying the model that is presented here. The basic theory and concepts remain the same, but some laborious algebraic evaluations will be required.

3.3.1.1 Notation and Definitions

With reference to Figure 3-2, the following notation and definitions will be used in the subsequent development:

- a Semimajor axis of the elliptic orbit
- e Eccentricity of this ellipse
- I Inclination of the orbit, angle YNP
- Ω Longitude of ascending node, angle XSN
- ω Argument of perigee, angle NSA
- f True anomaly, angle ASP
- T Orbital period, the time elapsing between successive passages through the pericenter
- τ Epoch, the time at which the body passes through the pericenter
- t The time at which the body is at some point P
- μ Universal gravitational constant
- η Mean motion of body: $\eta = \mu^{1/2} a^{-3/2}$ rad/sec
- M Mean anomaly: $M = \eta (t - \tau)$
- E Eccentric anomaly, defined by $M = E - e \sin E$
- Φ Celestial longitude of body, angle XZP
- θ Celestial latitude of body, angle CSP

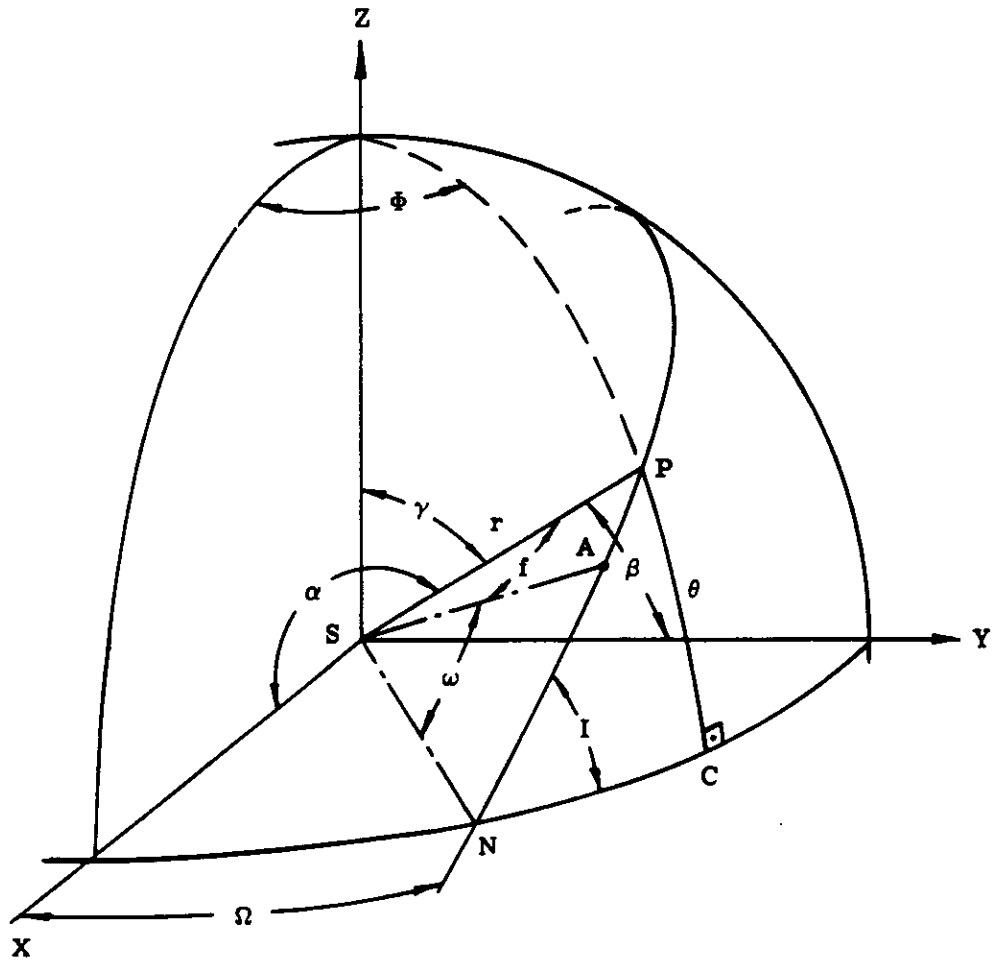


Fig. 3-2 — Orbital elements

3.3.1.2 Rectangular Coordinates (XYZ) of Body

The coordinates of P with respect to the inertial system are given by

$$\begin{bmatrix} X_0 \\ Y_0 \\ Z_0 \end{bmatrix} = \begin{bmatrix} A_x & B_x \\ A_y & B_y \\ A_z & B_z \end{bmatrix} \begin{bmatrix} \cos (E) - e \\ \sin E \end{bmatrix} \quad (3.1)$$

in which the matrix

$$\begin{bmatrix} A_x & B_x \\ A_y & B_y \\ A_z & B_z \end{bmatrix}$$

is given by

$$\begin{bmatrix} A_x & B_x \\ A_y & B_y \\ A_z & B_z \end{bmatrix} = a \begin{bmatrix} \cos \Omega & -\cos I \sin \Omega \\ \sin \Omega & \cos I \cos \Omega \\ 0 & \sin I \end{bmatrix} \begin{bmatrix} \cos \omega & -\sin \omega \\ \sin \omega & \cos \omega \end{bmatrix} \begin{bmatrix} 1 & 0 \\ 0 & (1-e^2)^{1/2} \end{bmatrix} \quad (3.2)$$

The positional coordinates given by Equation 3.2 are in an inertial system with reference to which the orbital elements are given. In order that they may be referred to some other coordinate system, transformations will be necessary. These transformations are specified in Section 3.5.4.

3.3.2 Camera Orientation

Stellar cameras, used in conjunction with the frame camera yield approximate values of the camera roll, pitch, and yaw. At the times of these exposures, the local horizon is equivalent to the tangent plane at the nadir point, which is defined as the point at which the position vector, \bar{r} , to the air station intersects the reference ellipsoid. The longitude, Φ_0 , and geocentric latitude, λ_0 , of the nadir are determined from

$$\begin{bmatrix} X_0 \\ Y_0 \\ Z_0 \end{bmatrix} = r \begin{bmatrix} \cos \Phi_0 \cdot \cos \lambda_0 \\ \cos \Phi_0 \cdot \sin \lambda_0 \\ \sin \Phi_0 \end{bmatrix} \quad (3.3)$$

according to

$$\lambda_0 = \cos^{-1} [(X_0)/(X_0^2 + Y_0^2)^{1/2}], \text{ for } X_0 \geq Y_0 \quad (3.4)$$

or

$$\lambda_0 = \sin^{-1} [(Y_0)/(X_0^2 + Y_0^2)^{1/2}], \text{ for } X_0 \leq Y_0 \quad (3.5)$$

and

$$\phi_0 = \tan^{-1} [(Z_0)/(X_0^2 + Y_0^2)^{-1/2}] \quad (3.6)$$

The orientation matrix rotating the ground coordinates into the photographic system may be expressed as:

$$R_j = \begin{bmatrix} \cos \kappa & \sin \kappa & 0 \\ -\sin \kappa & \cos \kappa & 0 \\ 0 & 0 & 1 \end{bmatrix} \begin{bmatrix} \cos \varphi & 0 & -\sin \varphi \\ 0 & 1 & 0 \\ \sin \varphi & 0 & \cos \varphi \end{bmatrix} \begin{bmatrix} 1 & 0 & 0 \\ 0 & \cos \omega_j & \sin \omega_j \\ 0 & -\sin \omega_j & \cos \omega_j \end{bmatrix} \quad (3.7)$$

The orientation between the local coordinate system and the geocentric terrestrial system is determined as:

$$O_j = \begin{bmatrix} \cos A_0 & -\sin A_0 & 0 \\ \sin A_0 & \cos A_0 & 0 \\ 0 & 0 & 1 \end{bmatrix} \begin{bmatrix} \sin \phi_0 & 0 & \cos \phi_0 \\ 0 & 1 & 0 \\ -\cos \phi_0 & 0 & \sin \phi_0 \end{bmatrix} \begin{bmatrix} -\cos \lambda_0 & -\sin \lambda_0 & 0 \\ \sin \lambda_0 & -\cos \lambda_0 & 0 \\ 0 & 0 & 1 \end{bmatrix} \quad (3.8)$$

Thus, the relationship between the photo-coordinates and the ground coordinates may be written as:

$$\begin{bmatrix} x_i - x_0 \\ y_i - y_0 \\ -f \end{bmatrix}_j = k (\kappa_j)(\varphi_j)(\omega_j)(A_0)(\phi_0)(\lambda_0) \begin{bmatrix} X_i - X_0 \\ Y_i - Y_0 \\ Z_i - Z_0 \end{bmatrix}_j \quad (3.9)$$

where k is an undetermined scalar. The values of all terms in Equation 3.9 pertain to a discrete time. For any specific time, t_0 , the corresponding terms may be evaluated and held constant in this manner. The dynamic local system may be transformed into a static one with reference to which subsequent computations may be performed for any time, t_i , provided that appropriate variations of \bar{X}_0 , due to orbital motion of ω_j , ϕ_j , and κ_j (due to capsule tumbling), and of \bar{X}_i , due to the earth's rotation, are applied.

This is accomplished through computing in the sidereal system. Denoting the orientation matrix $R_j O_j$ as M_j , Equation 3.9 may be rewritten as $\bar{x}_i = M_j \bar{X}_i$ from which the projective relationship

$$x_i = x_0 - f \frac{\begin{bmatrix} m_{11} (X_i - X_0) + m_{12} (Y_i - Y_0) + m_{13} (Z_i - Z_0) \\ m_{31} (X_i - X_0) + m_{32} (Y_i - Y_0) + m_{33} (Z_i - Z_0) \end{bmatrix}}{\begin{bmatrix} m_{31} (X_i - X_0) + m_{32} (Y_i - Y_0) + m_{33} (Z_i - Z_0) \end{bmatrix}} \quad (3.10)$$

and

$$y_i = y_0 - f \frac{\begin{bmatrix} m_{21} (X_i - X_0) + m_{22} (Y_i - Y_0) + m_{23} (Z_i - Z_0) \\ m_{31} (X_i - X_0) + m_{32} (Y_i - Y_0) + m_{33} (Z_i - Z_0) \end{bmatrix}}{\begin{bmatrix} m_{31} (X_i - X_0) + m_{32} (Y_i - Y_0) + m_{33} (Z_i - Z_0) \end{bmatrix}} \quad (3.11)$$

are obtained.

In these expressions, f is the camera focal length, m_{jk} is an element of the orientation matrix M_j , X_0, Y_0, Z_0 are the coordinates of the exposure station in the XYZ system, and $X_i, Y_i,$ and $Z_i,$ are the coordinates of the ground point corresponding to the image point $x_i, y_i, -f.$

These two equations are generalized for convenience into the form

$$F_{ki} = G_{ki} + f \left[\frac{m_{k1} (X_i - X_0) + m_{k2} (Y_i - Y_0) + m_{k3} (Z_i - Z_0)}{m_{31} (X_i - X_0) + m_{32} (Y_i - Y_0) + m_{33} (Z_i - Z_0)} \right] \quad (3.12)$$

where $k = 1, 2$

$$G_{1i} = x_i - x_0$$

$$G_{2i} = y_i - y_0$$

These two equations may be expressed in terms of the constituent variables $\omega_j, \phi_j, \kappa_j, A_0, \dots, Z_0.$ It is noted, however, that some of these are functionally related to the orbital parameters and to each other. The constrained solution must utilize independent parameters, as outlined in the subsequent section.

3.3.3 Constrained Solution

The functions given by Equation 3.12 express the relationship between a series of data consisting of observed variables and known and unknown various parameters. Those which are known are derived from observational data and are subject to the errors in these fundamental data.

On substituting the various parameters and data into Equation 3.12 the value of F_{ki} will be zero if, and only if, all entries are exact. The problem is to determine the most probable values for all parameters and variables. This is accomplished through a constrained least squares solution.

3.3.3.1 Least Squares Solution

Equation 3.12 is considered to be a function of the observed variables x_i and $y_i,$ and a function of the parameters $x_0, y_0, f, \omega_j, \phi_j, \kappa_j, \Omega, \omega, I, e, \eta, \tau, Y_j, X_j,$ and $Z_j.$

Consequently, rewrite Equation 3.12 as

$$F_{ki} = f_k (x_i, y_i; x_0, y_0, f; \omega_j, \phi_j, \kappa_j, \Omega, \omega, I, e, \eta, \tau; X_j, Y_j, Z_j) \quad (3.13)$$

Assuming that approximate values of these parameters are available, designated by a superscript $o,$ an approximate value of Equation 3.13 is obtained as

$$F_{ki}^o = f_k (x_i^o, y_i^o, \dots, X_i^o, Y_i^o, Z_i^o) \quad (3.14)$$

The true values of these items is obtained by applying a correction to these approximate values.

The reduced condition equation may be expressed in the form

$$A_x V_x + B_1 \Delta_1 + B_2 \Delta_2 + E_x = 0 \quad (3.15)$$

where V_x = vector of unknown residuals
 Δ_1 = vector of unknown parameter corrections
 Δ_2 = vector of unknown parameter corrections
 E_x = vector of random variables

and

$$A_x = \frac{\partial (F_1, F_2)_{ij}}{\partial (\text{observed variables})} = \frac{\partial (F_1, F_2)_{ij}}{\partial (x_1, y_1)_j} \quad (3.16)$$

$$B_1 = \frac{\partial (F_1, F_2)_{ij}}{\partial (\text{unknown parameters})} = \frac{\partial (F_1, F_2)_{ij}}{\partial (\text{all or none of } x_0, \dots, \tau)} \quad (3.17)$$

$$B_2 = \frac{\partial (F_1, F_2)_{ij}}{\partial (\text{parameters to be constrained})} = \frac{\partial (F_1, F_2)_{ij}}{\partial (\text{remaining parameters})} \quad (3.18)$$

assuming that a statistical estimate of, for example, q parameters are known, and that we wish to constrain the adjustment to fit these estimates, designate the statistical estimates of the q parameters $\bar{\beta}$ by

$$\bar{\beta}^0 = \begin{bmatrix} \beta_1^0 \\ \beta_2^0 \\ \vdots \\ \beta_q^0 \end{bmatrix} \quad (3.19)$$

having an associated covariance matrix σ_β

$$\sigma_\beta = \begin{bmatrix} \sigma_{\beta_1}^2 & \sigma_{\beta_1\beta_2} & \dots & \sigma_{\beta_1\beta_q} \\ \sigma_{\beta_2\beta_1} & \sigma_{\beta_2}^2 & \dots & \sigma_{\beta_2\beta_q} \\ \cdot & \cdot & \dots & \cdot \\ \cdot & \cdot & \dots & \cdot \\ \cdot & \cdot & \dots & \cdot \\ \sigma_{\beta_q\beta_1} & \sigma_{\beta_q\beta_2} & \dots & \sigma_{\beta_q}^2 \end{bmatrix} \quad (3.20)$$

New linear equations may be formed and solved with Equation 3.15, according to

$$\bar{\beta}^0 + \bar{V}^0\beta = \bar{\beta}^{00} + \bar{\Delta}_2 \quad (3.21)$$

where $\bar{\beta}^{00}$ = a current corrected value of $\bar{\beta}^0$
 \bar{V}^0 = an unknown residual vector

This equation is reformed as

$$\bar{V}_\beta - \bar{\Delta}_2 + \bar{G} = 0 \tag{3.22}$$

where $\bar{G} = \bar{\beta}^0 - \bar{\beta}^{00}$

Whence Equation 3.15 may be written as

$$A\bar{V} + B\bar{\Delta} + E = 0 \tag{3.23}$$

where

$$\bar{V} = \begin{bmatrix} V_x \\ V_\beta \end{bmatrix} \tag{3.24}$$

$$\bar{\Delta} = \begin{bmatrix} \Delta_2 \\ \Delta_1 \end{bmatrix} \tag{3.25}$$

$$E = \begin{bmatrix} E_x \\ G \end{bmatrix} \tag{3.26}$$

$$A = \begin{bmatrix} A_x & 0 \\ 0 & I_{qq} \end{bmatrix} \tag{3.27}$$

and

$$B = \begin{bmatrix} B_2 & B_1 \\ -I_{qq} & 0 \end{bmatrix} \tag{3.28}$$

The conditioned solution of Equation 3.23 for V and Δ which minimizes

$$S = V^T \sigma^{-1} V \tag{3.29}$$

is required, in which

$$\sigma = \begin{bmatrix} \sigma_x & 0 \\ 0 & \sigma_\beta \end{bmatrix} \tag{3.30}$$

where σ_x = the covariance matrix of the observed variables

The required solution is obtained from

$$S = V^T \sigma^{-1} V - 2\lambda^T (AV + B\Delta + E) \tag{3.31}$$

in which λ is a vector of Lagrangian multipliers, by setting $dS/dV = 0$ and $dS/d\Delta = 0$, to yield

$$V = \sigma A^T \lambda \tag{3.32}$$

and

$$-2B^T \lambda = 0 \tag{3.33}$$

which are combined with Equation 3.23 to yield

$$\lambda = -(A\sigma A^T)^{-1} (B\Delta + E) \tag{3.34}$$

and

$$\Delta = -[B^T(A\sigma A^T)^{-1} B]^{-1} B^T(A\sigma A^T)^{-1} E \tag{3.35}$$

This equation is evaluated by partitioning, the partitions being given by the following identities:

$$A\sigma A^T = \left[\begin{array}{c|c} A_x \sigma_x A_x^T & 0 \\ \hline 0 & \sigma_\beta \end{array} \right] \tag{3.36}$$

$$(A\sigma A^T)^{-1} = \left[\begin{array}{c|c} (A_x \sigma_x A_x^T)^{-1} & 0 \\ \hline 0 & \sigma_\beta^{-1} \end{array} \right] \tag{3.37}$$

$$B^T(A\sigma A^T)^{-1} B = \left[\begin{array}{c|c} B_2^T W_x B_2 + \sigma_\beta^{-1} & B_2^T W_x B_1 \\ \hline B_1^T W_x B_2 & B_1^T W_x B_1 \end{array} \right] \tag{3.38}$$

and

$$B^T(A\sigma A^T)^{-1} E = \left[\begin{array}{c} B_2^T W_x E_x - \sigma_\beta^{-1} G \\ \hline B_1^T W_x E_x \end{array} \right] \tag{3.39}$$

where

$$W_x = (A_x \sigma_x A_x^T)^{-1}$$

3.3.3.2 Application and Extension

In order to clarify the previous treatment, a descriptive example of applying these formulas to our problem is given.

For each photograph, j , one obtains for each point, i ,

$$A_i = \begin{bmatrix} \partial F_1 / \partial x_i & \partial F_1 / \partial y_i \\ \partial F_2 / \partial x_i & \partial F_2 / \partial y_i \end{bmatrix} \tag{3.40}$$

To each ground point that is known, a variance-covariance matrix may be assigned. For unknown ground points, coordinate values are estimated, together with large variances for these estimates.

Orbital parameters are estimated from the given ephemeris, and values of rotations ω_j , φ_j , and κ_j are determined from stellar cameras. Values for x_0 , y_0 , and f are obtained from calibration data.

The end result is that all parameters are to be constrained, dictating that $B_1 = 0$.

Consequently,

$$B_2 = \begin{bmatrix} \partial F_1/\partial x_0 & \partial F_2/\partial x_0 \\ \partial F_1/\partial y_0 & \partial F_2/\partial y_0 \\ \partial F_1/\partial f & \partial F_2/\partial f \\ \partial F_1/\partial \omega_j & \partial F_2/\partial \omega_j \\ \partial F_1/\partial \varphi_j & \partial F_2/\partial \varphi_j \\ \partial F_1/\partial \kappa_j & \partial F_2/\partial \kappa_j \\ \partial F_1/\partial \Omega & \partial F_2/\partial \Omega \\ \partial F_1/\partial \omega & \partial F_2/\partial \omega \\ \partial F_1/\partial I & \partial F_2/\partial I \\ \partial F_1/\partial e & \partial F_2/\partial e \\ \partial F_1/\partial n & \partial F_2/\partial n \\ \partial F_1/\partial \tau & \partial F_2/\partial \tau \\ \partial F_1/\partial X_1 & \partial F_2/\partial X_1 \\ \partial F_1/\partial Y_1 & \partial F_2/\partial Y_1 \\ \partial F_1/\partial Z_1 & \partial F_2/\partial Z_1 \end{bmatrix}^T \quad (3.41)$$

The various covariance matrices are:

- σ_{x_i} = the measured frame photograph images
- σ_{X_i} = the ground coordinates
- σ_c = the frame camera constants
- σ_α = the camera tilt angles

and

σ_o for the orbital elements

The two condition equations for each ground point image are:

$$A_i V_i + B_i \Delta_i + E_i = 0$$

where

$$A_i = \left[\begin{array}{c|c} A_{xi} & 0 \\ \hline (2 \times 2) & (2 \times 15) \\ \hline 0 & I \\ \hline (15 \times 2) & (15 \times 15) \end{array} \right] \quad (3.42)$$

Now,

$$V_i = (V_{xi}, V_{yi}, \dots, V_{\tau}, V_{Xi}, V_{Yi}, V_{Zi})^T \quad (3.43)$$

$$B_i = \left[\begin{array}{c} B_2 \\ \hline (2 \times 15) \\ \hline -I \\ \hline (15 \times 15) \end{array} \right] \quad (3.44)$$

$$\Delta_i = (\delta_{x0}, \delta_{y0}, \delta f, \dots, \delta Z_i)^T \quad (3.45)$$

and

$$E_i = (E_{xi}, E_{yi}, \dots, E_{Zi})^T \quad (3.46)$$

The associated weight matrix is

$$\sigma^{-1} = \text{Diagonal} (\sigma_{xi}, \sigma_c, \sigma_o, \sigma_{\alpha}, \sigma_{Xi})^{-1} \quad (3.47)$$

On forming the normal equations, rewritten as

$$N\Delta = -C, \text{ one obtains}$$

$$N = \sum B_i^T (A_i \sigma A_i^T)^{-1} B_i \quad (3.48)$$

and

$$C = \sum B_i^T (A_i \sigma A_i^T)^{-1} E_i \quad (3.49)$$

from which the solution for Δ is obtained as

$$\Delta = -N^{-1} C \quad (3.50)$$

If one reconsiders the normal equations, it is found that they consist of two parts—one pertaining to the orbital and camera parameter data, and one relating to the ground point data.

Following the notation and derivation of Brown, the observation Equation 3.23 may be rewritten in the form

$$AV + \dot{B}\delta + \ddot{B}\ddot{\delta} + E = 0 \tag{3.51}$$

where $\dot{B}, \dot{\delta}$ refer to orbital and camera parameters
 $\ddot{B}, \ddot{\delta}$ refer to the ground point data

Equation 3.37 may be rewritten in the form

$$W = (A\sigma A^T)^{-1} = \begin{bmatrix} W_x & 0 & 0 \\ 0 & \dot{W} & 0 \\ 0 & 0 & \ddot{W} \end{bmatrix} = \begin{bmatrix} (A_x\sigma_x A_x^T)^{-1} & 0 & 0 \\ 0 & (\dot{\sigma})^{-1} & 0 \\ 0 & 0 & (\ddot{\sigma})^{-1} \end{bmatrix} \tag{3.52}$$

where $\dot{\sigma}$ = diagonal $(\sigma_c, \sigma_o, \sigma_\alpha)$
 $\ddot{\sigma}$ = diagonal $(\sigma_{X1}, \sigma_{X2}, \dots, \sigma_{Xi})$

Equation 3.5 is equivalent to

$$W = \begin{bmatrix} A & 0 & 0 \\ 0 & I & 0 \\ 0 & 0 & I \end{bmatrix} \begin{bmatrix} \sigma_x^{-1} & 0 & 0 \\ 0 & \dot{W} & 0 \\ 0 & 0 & \ddot{W} \end{bmatrix} \begin{bmatrix} A^T & 0 & 0 \\ 0 & I & 0 \\ 0 & 0 & I \end{bmatrix}$$

Similarly Equation 3.38 may be rewritten as

$$\begin{aligned} N = B^T W B &= \begin{bmatrix} \dot{B}^T & -I & 0 \\ \ddot{B}^T & 0 & -I \end{bmatrix} \begin{bmatrix} W_x & 0 & 0 \\ 0 & \dot{W} & 0 \\ 0 & 0 & \ddot{W} \end{bmatrix} \begin{bmatrix} \dot{B} & \ddot{B} \\ -I & 0 \\ 0 & I \end{bmatrix} \\ &= \begin{bmatrix} (\dot{B}^T W_x \dot{B} + \dot{W}) & (\dot{B}^T W_x \ddot{B}) \\ (\ddot{B}^T W_x \dot{B}) & (\ddot{B}^T W_x \ddot{B} - \ddot{W}) \end{bmatrix} = \begin{bmatrix} \dot{N} + \dot{W} & N \\ \ddot{N}^T & \ddot{N} + \ddot{W} \end{bmatrix} \end{aligned} \tag{3.53}$$

Similarly, Equation 3.39 becomes

$$C = B^T W E = \begin{bmatrix} \dot{B}^T & -I & 0 \\ \ddot{B}^T & 0 & -I \end{bmatrix} \begin{bmatrix} W_x & 0 & 0 \\ 0 & \dot{W} & 0 \\ 0 & 0 & \ddot{W} \end{bmatrix} \begin{bmatrix} E_x \\ \dot{E} \\ \ddot{E} \end{bmatrix}$$

or

$$C = \begin{bmatrix} (\dot{B}^T W_x E_x - \dot{W} \dot{E}) \\ (\ddot{B}^T W_x E_x - \ddot{W} \ddot{E}) \end{bmatrix} = \begin{bmatrix} \dot{C} - \dot{W} \dot{E} \\ \ddot{C} - \ddot{W} \ddot{E} \end{bmatrix} \tag{3.54}$$

The normal equations, $N\Delta = -C$ are thus:

$$\begin{bmatrix} \dot{N} + \dot{W} & N \\ \bar{N}^T & \bar{N} + \bar{W} \end{bmatrix} \begin{bmatrix} \delta \\ \bar{\delta} \end{bmatrix} = - \begin{bmatrix} \dot{C} - \dot{W}\dot{E} \\ \bar{C} - \bar{W}\bar{E} \end{bmatrix} \quad (3.55)$$

which for computational purposes is partitioned

$$\begin{bmatrix} \dot{N} + \dot{W} & N_1 & N_2 & \dots & N_i \\ \bar{N}_1^T & \bar{N}_1 + \bar{W}_1 & & & \\ \bar{N}_2^T & & \bar{N}_2 + \bar{W}_2 & & \\ & & & & \\ \bar{N}_i^T & & & & \bar{N}_i + \bar{W}_i \end{bmatrix} \begin{bmatrix} \delta \\ \delta_1 \\ \delta_2 \\ \vdots \\ \delta_i \end{bmatrix} = \begin{bmatrix} \dot{C} - \dot{W}\dot{E} \\ \bar{C}_1 - \bar{W}_1\bar{E}_1 \\ \bar{C}_2 - \bar{W}_2\bar{E}_2 \\ \vdots \\ \bar{C}_i - \bar{W}_i\bar{E}_i \end{bmatrix} \quad (3.56)$$

Let $N^{-1} = M$, according to

$$\begin{bmatrix} \dot{N} + \dot{W} & N \\ \bar{N}^T & \bar{N} + \bar{W} \end{bmatrix}^{-1} = \begin{bmatrix} \dot{M} & \dot{M} \\ \bar{M}^T & \bar{M} \end{bmatrix} \quad (3.57)$$

Since $NM = I$, then, noting that $M = -\dot{M} N (\dot{N} + \dot{W})^{-1}$, one obtains

$$\dot{M} = [(\dot{N} + \dot{W}) - \bar{N} (\bar{N} + \bar{W})^{-1} \bar{N}^T]^{-1} \quad (3.58)$$

and

$$\bar{M} = [(\bar{N} + \bar{W})^{-1} + (\bar{N} + \bar{W})^{-1} \bar{N}^T \dot{M} \bar{N} (\bar{N} + \bar{W})^{-1}] \quad (3.59)$$

In order to determine the corrections δ and $\bar{\delta}$, it is not necessary to solve Equation 3.59. Consider

$$\begin{bmatrix} -\delta \\ -\bar{\delta} \end{bmatrix} = \begin{bmatrix} \dot{M} & \dot{M} \\ \bar{M}^T & \bar{M} \end{bmatrix} \begin{bmatrix} \dot{C} - \dot{W}\dot{E} \\ \bar{C} - \bar{W}\bar{E} \end{bmatrix} \quad (3.60)$$

from which

$$-\delta = [\dot{M} (\dot{C} - \dot{W}\dot{E}) + \bar{M} (\bar{C} - \bar{W}\bar{E})]$$

and

$$-\bar{\delta} = [\bar{M}^T (\dot{C} - \dot{W}\dot{E}) + \bar{M} (\bar{C} - \bar{W}\bar{E})]$$

Putting

$$Q = (\bar{N} + \bar{W})^{-1} \bar{N}^T \tag{3.61}$$

then

$$\bar{M} = -\dot{M} Q$$

and

$$-\dot{\delta} = \dot{M} [\dot{C} - \dot{W}\dot{E} - Q (\bar{C} - \bar{W}\bar{E})] \tag{3.62}$$

Since

$$-[\bar{N}^T \dot{\delta} + (\bar{N} + \bar{W}) \bar{\delta}] = \bar{C} - \bar{W}\bar{E}$$

then

$$-(\bar{\delta}) = (\bar{N} + \bar{W})^{-1} (\bar{C} - \bar{W}\bar{E}) - Q\dot{\delta} \tag{3.63}$$

It is to be noted that $\bar{N} + \bar{W}$ consists of i diagonally arranged 3×3 matrices, and consequently presents no difficulties.

3.3.3.3 Error Propagation

In the final iteration

$$V_x = E_x - \dot{B}\dot{\delta} - \bar{B}\bar{\delta}$$

$$\dot{V} = \dot{E} - \dot{\delta}$$

and

$$\bar{V} = \bar{E} - \bar{\delta}$$

with $\dot{\delta}$ and $\bar{\delta}$ tending to zero; i.e.,

$$V_x \rightarrow E_x$$

$$\dot{V} \rightarrow \dot{E}$$

$$\bar{V} \rightarrow \bar{E}$$

Now

$$S = V_x^T W_x V + \dot{V}^T \dot{W} \dot{V} + \bar{V}^T \bar{W} \bar{V} \tag{3.64}$$

which when divided by the degrees of freedom gives the unit variance σ_0 .

\bar{M} is the covariance matrix of the adjusted camera and orbital parameters, and \dot{M} is that of the ground points. It is to be noted that $\dot{M} = (\dot{N} + \dot{W})^{-1} + Q\dot{M}Q^T$, so that the covariance matrix of any point g is

$$\bar{M}_g = (\bar{N}_g + \bar{W}_g)^{-1} + Q_g \dot{M}_g Q_g^T \tag{3.65}$$

3.3.3.4 Auxiliary Data

Suppose auxiliary data, independent of the camera system, has been collected, which may be expressed as a function of the various parameters. As an example, a radar altimeter will indicate the value of nadiral distance, which may be expressed in terms of the orbital parameters.

Denote the vector of auxiliary data as Λ , which may be written as

$$\Lambda_h = F_h(\Omega, \omega, \dots, \tau) \tag{3.66}$$

then, as before

$$\Lambda_h = \Lambda_h^0 + V_{\Lambda h} \tag{3.67}$$

The various parameters $\alpha_p = (\Omega, \omega, \dots, \tau)$ may be expressed as

$$\alpha_p = \alpha_p^0 + \delta\alpha_p \tag{3.68}$$

so that

$$V_{\Lambda h} - \Lambda_{h1} \delta\alpha_1 - \dots - \Lambda_{hp} \delta\alpha_p = E_{\Lambda h} \tag{3.69}$$

where

$$E_{\Lambda h} = F_h(\alpha_1^0, \alpha_2^0, \dots, \alpha_p^0) \tag{3.70}$$

Consequently, an additional series of equations may be written as follows:

$$V_{\Lambda} - \Lambda \delta = E_{\Delta} \tag{3.71}$$

which, together with the covariance matrix of Λ , may be incorporated into the previous solution, according to

$$\begin{bmatrix} V_x \\ V_{\Lambda} \\ \dot{V} \\ \ddot{V} \end{bmatrix} + \begin{bmatrix} \dot{B} & \ddot{B} \\ -\Lambda & 0 \\ -I & 0 \\ 0 & I \end{bmatrix} \begin{bmatrix} \delta \\ \ddot{\delta} \end{bmatrix} = \begin{bmatrix} E_x \\ E_{\Delta} \\ \dot{E} \\ \ddot{E} \end{bmatrix} \tag{3.72}$$

to yield

$$N = \begin{bmatrix} (\dot{B}^T W_x \dot{B} + \dot{W} + \Lambda^T W_\Lambda \Lambda) & \dot{B}^T \bar{W} \bar{B} \\ \bar{B}^T W_x \dot{B} & (\bar{B}^T W_x \bar{B} + \bar{W}) \end{bmatrix} = \begin{bmatrix} \dot{N} + \dot{W} + \Lambda^T W_\Lambda \Lambda^T & \bar{N} \\ \bar{N}^T & \bar{N} + \bar{W} \end{bmatrix} \quad (3.73)$$

and

$$C = \begin{bmatrix} \dot{C} - \dot{W} \dot{E} - \Lambda W_\Lambda E_\Lambda \\ \bar{C} - \bar{W} \bar{E} \end{bmatrix} \quad (3.74)$$

Similarly, auxiliary data pertaining to ground point data, (X_1, Y_1, Z_1) might be used to exploit the relationship between auxiliary data and the various parameters.

3.3.4 Detailed Formulation

It is considered unnecessary to present the detailed expressions for individual elements of the various matrices and for the partial derivatives. This is due to the means by which these items will be obtained in a computational sequence, namely, by appropriate matrix manipulations. Furthermore, the final mathematical model will not be as simple as that used in this analysis. However, it is considered worthwhile to present the salient formulas, and the expressions from which the complete set of partial derivatives can be obtained.

The orientation matrix $M_j = R_j O_j$ is obtained from the multiplication of six matrices, according to Equations 3.7, 3.8, and 3.9. From Equation 3.12, the partial derivatives are obtained that are defined by Equations 3.16, 3.17, and 3.18 as

$$\left. \begin{array}{ll} \partial F_1 / \partial x_1 = 1 & \partial F_2 / \partial x_1 = 0 \\ \partial F_1 / \partial y_1 = 0 & \partial F_2 / \partial y_1 = 1 \\ \partial F_1 / \partial x_0 = -1 & \partial F_2 / \partial x_0 = 0 \\ \partial F_1 / \partial y_0 = 0 & \partial F_2 / \partial y_0 = -1 \\ \partial F_1 / \partial f = U_1 / W_1 & \partial F_2 / \partial f = V_1 / W \end{array} \right\} \quad (3.75)$$

where

$$\begin{bmatrix} U_1 \\ V_1 \\ W_1 \end{bmatrix} = M \begin{bmatrix} X_1 - X_0 \\ Y_1 - Y_0 \\ Z_1 - Z_0 \end{bmatrix} \quad (3.76)$$

Working in the sidereal time system, so that the values of $X_1, Y_1,$ and Z_1 are replaced by the value values $X_{1s}, Y_{1s},$ and Z_{1s} at time t_1 according to